AIP | The Journal of Chemical Physics

Thermal conductivity of carbon dioxide from non-equilibrium molecular dynamics: A systematic study of several common force fields

Thuat T. Trinh, Thijs J. H. Vlugt, and Signe Kjelstrup

Citation: The Journal of Chemical Physics **141**, 134504 (2014); doi: 10.1063/1.4896965
View online: http://dx.doi.org/10.1063/1.4896965
View Table of Contents: http://scitation.aip.org/content/aip/journal/jcp/141/13?ver=pdfcov
Published by the AIP Publishing

Thermal conductivity of carbon dioxide from non-equilibrium molecular dynamics: A systematic study of several common force fields

Thuat T. Trinh,[1] Thijs J. H. Vlugt,[2] and Signe Kjelstrup[1,2,a)]
[1]*Department of Chemistry, Norwegian University of Science and Technology, Trondheim, Norway*
[2]*Department of Process and Energy, Delft University of Technology, Delft, Netherlands*

(Received 16 July 2014; accepted 22 September 2014; published online 3 October 2014)

We report a systematic investigation of the thermal conductivity of various three-site models of carbon dioxide (CO_2) using nonequilibrium molecular dynamics in the temperature range 300–1000 K and for pressures up to 200 MPa. A direct comparison with experimental data is made. Three popular CO_2 force fields (MSM, EPM2, and TraPPE) and two flexible models (based on EPM2) were investigated. All rigid force fields accurately predict the equation of state for carbon dioxide for the given range of variables. They can also reproduce the thermal conductivity of CO_2 at room temperature and predict a decrease of the thermal conductivity with increasing temperature. At high temperatures, the rigid models underestimate the thermal conductivity. [http://dx.doi.org/10.1063/1.4896965]

I. INTRODUCTION

Carbon dioxide (CO_2) has an important impact on the climate and is therefore widely studied. Huge efforts are being made, for instance, to reduce emissions of CO_2 to the atmosphere, by capture- and sequestration techniques.[1,2] In that context, membrane separation techniques are needed, at high as well as low temperatures.[3,4] Fossil-fueled power systems, natural gas processes, or production of hydrogen gas include all high-temperature separation technologies.[2,5] The thermal conductivity of CO_2 is needed for process modelling in these processes.

Molecular simulation is a popular technique for the prediction of thermal conductivities of fluids.[6] The thermal conductivity of CO_2 has been calculated with various models, by using both equilibrium and non-equilibrium simulations.[7–9] Nieto-Draghi *et al.* used semi or fully flexible models of CO_2 to predict the thermal conductivity in the temperature range 300–400 K.[7] More recently Liang *et al.* showed that a CO_2 model with site-site interactions fitted from *ab initio* calculations provides a good prediction of the thermal conductivity at low density.[9] Most of these studies focused on a narrow temperature and pressure range (around room temperature and up to 10 MPa), while experimental data of the thermal conductivity of CO_2 are also available at elevated temperatures, and for pressures up to 1000 K and 200 MPa.[10] Hence, it is important to develop further a molecular dynamics simulation model for the thermal conductivity of this important molecule. A linear rigid model containing three interaction sites is commonly used for CO_2 in adsorption and diffusion studies of gas mixtures of CO_2 in various materials.[11–16] The quality of these rigid models of CO_2 for the prediction of thermal conductivity has not been reported, however.

In this work, we report thermal conductivities of CO_2 for the temperature range 300–1000 K and for pressures up to 200 MPa. We will use three common models of CO_2, namely, MSM,[17] EPM2,[18] and TraPPE,[19] and compare the computed conductivities with those of the National Institute of Standards and Technology database (NIST).[10] The models differ in their bonds lengths of C–O and in their values of the Lennard-Jones (LJ) potential parameters, as well as in the partial charges that are used. We will show that all rigid models can correctly predict the thermal conductivity of CO_2. The TraPPE model is slightly superior. However, at high temperatures all models underestimate the thermal conductivity of CO_2. In order to understand why, two flexible models, based on EPM2, will also be examined. We shall see that flexibility may partially explain the discrepancy observed.

The paper is structured as follows. In Sec. II, an overview of the technical and simulation details is provided. The predictions of the equation of state are presented in Sec. III. The thermal conductivity of CO_2 at various pressures and temperatures from the various models are next compared with the experimental data from NIST. We will close the paper in Sec. IV with comments and conclusions.

II. SIMULATION DETAILS

All models for CO_2 studied here are 3-site models with fixed C=O bond length and a fixed angle of 180°. Only intermolecular interactions are needed to describe the system. The intermolecular potential consists of long-range Coulombic interactions, and a shifted and truncated 12-6 LJ potential[20]

$$V_{ij}^{nb} = V_{ij}^{LJ} + V_{ij}^{coulombic}, \tag{1}$$

$$V_{ij}(r_{ij}) = 4\varepsilon_{ij}\left[\left(\frac{\sigma_{ij}}{r_{ij}}\right)^{12} - \left(\frac{\sigma_{ij}}{r_{ij}}\right)^{6}\right], \tag{2}$$

a)Author to whom correspondence should be addressed. Electronic mail: signe.kjelstrup@ntnu.no

TABLE I. Parameters of several CO_2 potential models used in simulations. The flexible models were based on EPM2 model with additional bond stretching and angle bending terms. The EPM2_Flex2 was fitted in this work based on quantum calculation (Figure 1).

Models	ε_C (K)	σ_C (Å)	ε_O (K)	σ_O (Å)	q_C (e)	q_O (e)	d_{C-O} (Å)
MSM[17]	29.00	2.79	83.10	3.01	0.60	−0.298	1.16
EPM2[18]	28.13	2.76	80.51	3.03	0.65	−0.326	1.15
TraPPE[19]	27.00	2.80	79.00	3.05	0.70	−0.350	1.16
EPM2_Flex1[7,18]	$k_S = 10739$ kJ/mol Å^2 (Ref. 7)				$k_B = 1236$ kJ/mol rad^2 (Ref. 17)		
EPM2_Flex2 (Refs. 7, 18, this work)	$k_M = 2015.75$ kJ/mol Å^2, $\alpha = 2.35$				$k_B = 1236$ kJ/mol rad^2 (Ref. 17)		

$$V_{ij}^{LJ}(r_{ij}) = \begin{cases} V_{ij}(r_{ij}) - V_{ij}(r_c) & r_{ij} < r_c, \\ 0 & r_{ij} > r_c \end{cases}, \quad (3)$$

where r_{ij} is the distance between atoms i and j, ε_{ij} and σ_{ij} are LJ potential parameters, and r_c is the cutoff radius. The LJ interaction parameters between different types of atoms were calculated from the Lorentz-Berthlot mixing rules[20]

$$\varepsilon_{ij} = \sqrt{\varepsilon_{ii}\varepsilon_{jj}}, \quad (4)$$

$$\sigma_{ij} = \frac{1}{2}(\sigma_{ii} + \sigma_{jj}). \quad (5)$$

The Coulombic interactions equal

$$V_{ij}^{coulombic} = \frac{1}{4\pi\varepsilon_0}\frac{q_i q_j}{r_{ij}}, \quad (6)$$

where q_i, q_j are the partial charges on atoms i, j, and ε_0 is the dielectric constant of vacuum. In our work, we used the particle-particle particle-mesh solver implemented in LAMMPS[21] for electrostatic interactions, see Ref. 22 for more details. The force field parameters for the MSM,[17] EPM2,[18] and TraPPE[19] models are listed in Table I. They were determined at room temperature to reproduce liquid vapor equilibrium of CO_2.

For the fully flexible models (EPM2_Flex1, EPM2_flex2), additional functions were used to describe bond stretching (harmonic potential Eq. (7) or Morse potential Eq. (8)) and angle bending of CO_2 (Eq. (9))

$$V_S(r_{ij}) = \frac{1}{2}k_S(r_{ij} - r_0)^2, \quad (7)$$

$$V_M(r_{ij}) = k_M[1 - e^{-\alpha(r_{ij}-r_0)}]^2, \quad (8)$$

$$V_B(\theta_{ijk}) = \frac{1}{2}k_B(\theta_{ijk} - \theta_0)^2, \quad (9)$$

where r_{ij} is the distance between atom i and j; θ_{ijk} is the angle between atoms i,j,k; k_S and k_B are the force constant. The nonbonding parameters for the MSM,[17] EPM2,[18] and TraPPE[19] models force fields are also listed in Table I. For flexible models k_B was taken from Harris and Yung.[18] In EMP2_flex1, k_S was taken from Nieto-Draghi *et al.*[7] using harmonic potential for C–O bond stretching; however, the harmonic equation (7) was not able to describe the separation of atoms at longer distance.[6] Hence, a Morse potential for EPM2_flex2 was fitted with Eq. (8) using quantum chemistry data to overcome this limitation of harmonic potential. We used Gaussian 09 package[23] to perform a Density Functional Theory (DFT) calculation with B3LYP functional[24,25] and a full-electron 6-311+G(d,p) basis set.[26] Geometry optimization and potential energy scan was made to fit with a Morse potential (Figure 1).

The cut-off radius was 12 Å, which corresponds to $r_{cut} \sim 4\sigma_O$. The tail correction was not used for this cut-off. An increase of the cut-off value in our simulations, did not improve the accuracy of the computed thermal conductivity of CO_2, but significantly increased the computational cost.[27] It was observed by Bugel and Galliero for Lennard-Jones fluids that $r_{cut} = 2.5\sigma$ was sufficient for reliable results for thermal conductivity.[28]

The thermal conductivity can be either obtained from equilibrium molecular dynamics (EMD) or from non-equilibrium molecular dynamics (NEMD) simulations.[20] The Green-Kubo formulations are commonly used in EMD to access the thermal conductivity. There are several NEMD techniques to obtain a heat flux and the corresponding temperature gradient, from which the thermal conductivity is computed. The non-equilibrium situation can be obtained by swapping particle momenta,[29,30] by using a heat exchange algorithm (HEX),[31] or by thermostating the boundaries.[32,33] In this work, we applied the thermostating technique, which was used earlier to successfully calculate the thermal conductivity of hydrocarbons[32,34] in zeolites and water.[33] Here, we summarize the essentials of the simulation technique, previously

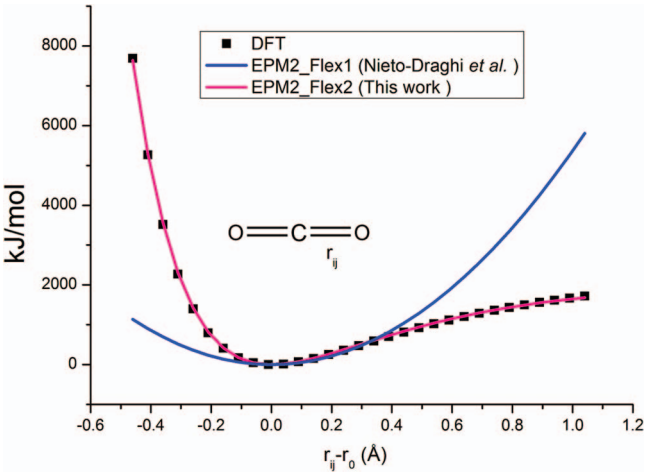

FIG. 1. Energy potential of CO_2 bond stretching calculated by DFT B3LYP/6-311+G(d,p). The continuous line represents a harmonic potential Eq. (7) by Nieto-Draghi *et al.*[7] and Morse potential Eq. (8) (this work). The parameters are in Table I.

described in Refs. 32 and 33. We took a simulation box size of 20 × 3 × 3 (nm^3) with periodic boundary conditions in three dimensions. The total number of CO_2 molecules was in the range 200–3000 to cover a wide range of densities, from 80 to 1200 kg/m^3. In total, 300 simulations were performed to compute the thermal conductivity of CO_2 in the temperature range 300 K–1000 K for the four different CO_2 models. The time step for integration of the equations of motion was 1 fs. The initial configuration was constructed by randomly distributing the CO_2. The system was stabilized during 1 ns by *NVT* runs with the Nosé-Hoover thermostat.[35] When the system was in thermal equilibrium, we performed NEMD simulations of 5 ns runs in the microcanonical ensemble (*NVE*) with thermostats[6] at the hot and cold regions. A longer run of 7.5 ns was performed at high temperature (600–1000 K). The heat flux and temperature gradient were checked for convergence. The average values of temperature and pressure in NEMD simulations were within 1% of expected values. The last 2.5 ns of the run was used to determine the temperature gradient and the heat flux through the system. This is sufficiently long to obtain sufficient statistics and consistent trajectories. The simulation temperature was set as $T = \frac{1}{2}(T_{\text{cold}} + T_{\text{hot}})$. The simulation box was divided into 20 small equal slabs. The cold and hot regions were chosen in slabs 1–2 and slabs 11–12, respectively. The volumes of the cold and hot regions are the same along the x-direction of the simulation box (Figure 1). In the NEMD simulation, the average temperature of each slab was recorded. The temperature gradient was obtained by fitting all average temperatures along the x-axis to a straight line, excluding the thermostat regions.

The temperature was maintained in each thermostat by supply or withdrawal of kinetic energy. The total energy of the system is unchanged, meaning that the energy withdrawn is the energy supplied. The heat (energy) flux through the system can therefore be computed from the change in kinetic energy $\langle K \rangle$ in any of the two thermostats during a single time step

$$J_q = \frac{\langle K \rangle}{2 \times \delta t \times A}, \tag{10}$$

where J_q is the heat flux through the simulation box, δt is the time step, and A is the cross sectional area. The factor 2 arises from the fact that due to the periodic boundary conditions that there are two temperature gradients in the symmetric simulation box. The thermal conductivity is obtained from Fourier's law (11)

$$J_q = -\lambda \Delta T. \tag{11}$$

In order to compare with experimental data, we used the root mean squared error of a model, defined as

$$\text{RMSE} = \text{sqrt}\left(\sum_{i=1}^{k} (\lambda_{sim} - \lambda_{\text{exp}})^2 / k\right), \tag{12}$$

where λ_{sim}, λ_{exp}, and k are the calculated thermal conductivity, experimental thermal conductivity, and number of simulations, respectively. The minimum error (%) is defined as

$$\text{Err}(\%) = \frac{\text{RMSE}}{\lambda_{\text{exp}}^{\max}} \times 100\%. \tag{13}$$

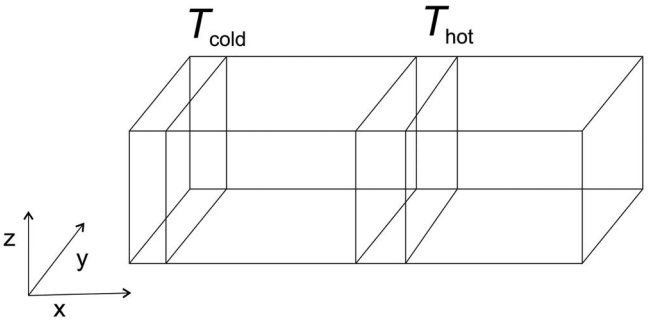

FIG. 2. The NEMD simulations to apply temperature gradient in the simulation box. See text for details.

The relative error is defined as

$$\Delta\lambda = \frac{\lambda_{sim} - \lambda_{\text{exp}}}{\lambda_{\text{exp}}} \times 100\%. \tag{14}$$

III. RESULTS AND DISCUSSIONS

We investigated first 120 state points, in order to generally assess the CO_2-models. The average temperature in the simulation box varied from 300 K to 1000 K, while the pressure was varied up to 200 MPa. The models were first tested for their accuracy in the prediction of the equation of state for CO_2. Figure 2 shows the pressure and density obtained for various temperatures together with the NIST experimental data.[10] All models reproduced very well the thermodynamic equation of state, at low as well as high temperatures and pressures. Calculated points fell almost on top of each other. In spite of the CO_2 models being developed to fit experimental data below the critical temperature (for vapor-liquid phase equilibria of pure CO_2 and CO_2 in mixtures with hydrocarbons), a very good prediction was found for the equation of state of CO_2, also at higher temperatures. The flexible model created here, gives an equally good prediction at low

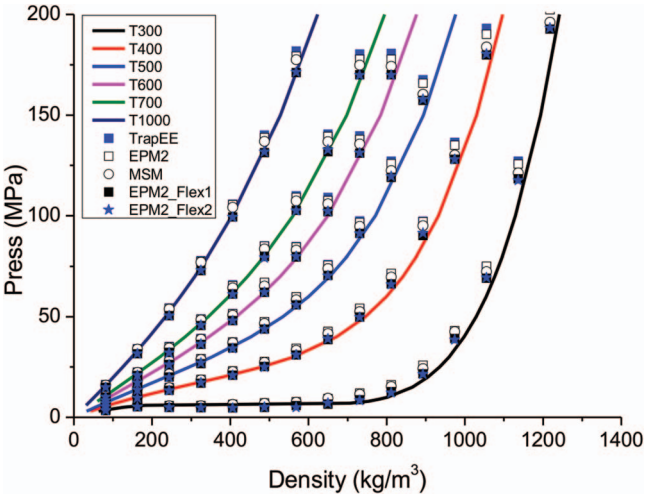

FIG. 3. Equation of state of CO_2 for various temperatures in the interval 300 K–1000 K. Four different CO_2 models are reported (see text for explanation). The solid lines represent experimental data taken from the NIST database.[10]

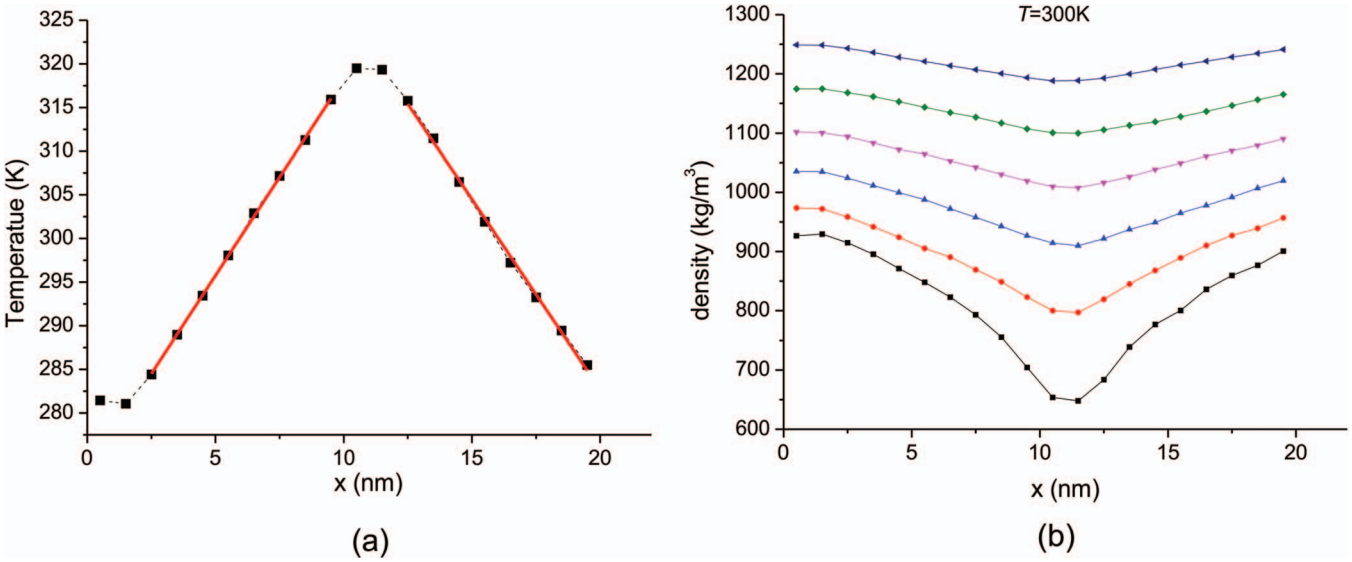

FIG. 4. (a) A typical average temperature profile in the simulation box at an average temperature of 300 K and $N_{CO2} = 3000$. (b) An average density profile from NEMD simulations at 300 K at various densities.

pressure, but slightly better at high pressure (Figure 3). An average error (defined by Eq. (13)) is 6.3% and 3.6% for rigid and flexible models, respectively. The NEMD simulations to calculate the thermal conductivity of CO_2 were therefore done with all models.

The microstructure of CO_2 was previously studied by *ab initio* molecular dynamics and flexible model.[36] The radial distribution functions and distribution of bond and angle of CO_2 obtained by flexible models (see the supplementary material[27]) are in agreement with literature.[36] At high temperature 1000 K, the bond angles are more flexible than that at 300 K. However, both bond length and angle distribution obtained by flexible classical force field are more rigid than that obtained by *ab initio* results.[36]

Figure 4 shows the average temperature and density profile of a typical run at T = 300 K with the TraPPE force field. We obtain similar profiles for the MSM, EPM2, and flexible models (not shown). The temperature profile was fitted to a straight line positioned in the analysis layers (discarding the hot and cold regions). A good accuracy fit was obtained for all temperatures (regression coefficient $R^2 > 0.90$). The temperature gradient was typical chosen in range 3–5 K nm^{-1}. Larger gradients have been selected earlier (e.g., 15–20 K(nm)$^{-1}$ for water[33]). We verified that the magnitude of the temperature gradient does not influence the value of the thermal conductivity.[28] The intermolecular potential parameter of the model is the most important factor in its determination. Typical results from the TraPPE model at 300 K and various densities are listed in Table II. The error bar (the estimate is based on the error bar of heat flux and temperature gradient) of the calculated thermal conductivity is maximum 5 mW m^{-1} K^{-1}. The simulated value predicted the

TABLE II. Thermal conductivity of carbon dioxide from the TraPPE model at 300 K as a function of density. The symbols λ_{sim}, λ_{exp} denote the thermal conductivity from simulations and from the NIST data of Ref. 10, respectively. ΔT is the temperature gradient. J_q is the heat flux through the system.

N_{CO2}	density (kg/m^3)	ΔT (K nm^{-1})	J_q (10^8 W m^{-2})	λ_{sim} (mW m^{-1} K^{-1})	λ_{exp} (mW m^{-1} K^{-1})	$\Delta\lambda$ (%)
200	81.19	−3.31 ± 0.32	0.4743 ± 0.0001	14 ± 1	20	− 30
400	162.38	−4.03 ± 0.14	0.8549 ± 0.0002	21 ± 1	28	− 25
600	243.57	−5.07 ± 0.21	0.9772 ± 0.0004	19 ± 1	24	− 19
800	324.76	−3.98 ± 0.25	1.0948 ± 0.0004	28 ± 2	25	9
1000	405.94	−4.05 ± 0.33	1.2133 ± 0.0006	30 ± 2	27	10
1200	487.13	−3.82 ± 0.29	1.4557 ± 0.0004	38 ± 3	36	7
1400	568.32	−3.34 ± 0.25	1.9962 ± 0.0005	60 ± 5	73	− 18
1600	649.51	−3.57 ± 0.17	2.7451 ± 0.0004	77 ± 4	85	− 10
1800	730.70	−4.19 ± 0.10	3.2565 ± 0.0005	78 ± 2	91	− 15
2000	811.89	−4.20 ± 0.10	4.2357 ± 0.0004	101 ± 3	99	2
2200	893.08	−4.22 ± 0.08	4.9672 ± 0.0004	118 ± 2	112	5
2400	974.27	−4.38 ± 0.03	5.777 ± 0.0004	132 ± 1	131	<1
2600	1055.45	−4.36 ± 0.06	7.0228 ± 0.0004	161 ± 2	155	4
2800	1136.64	−4.54 ± 0.07	8.1799 ± 0.0005	180 ± 3	185	− 3
3000	1217.83	−4.43 ± 0.04	10.0376 ± 0.0004	226 ± 2	...	...

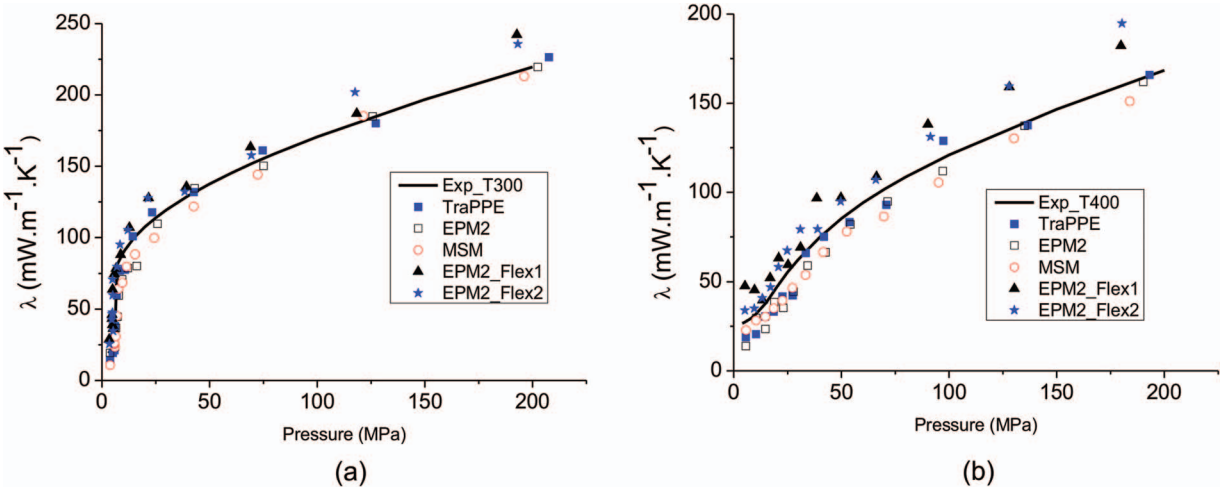

FIG. 5. Calculated thermal conductivity of rigid models (TraPPE, EPM2, MSM) and fully flexible models (EPM2_Flex1, EPM2_flex2) at T = 300 K (a) and T = 400 K (b). The straight line is experimental data taken from NIST data.[10]

experimental result within this accuracy at medium densities. The deviation between the two was relatively larger at low densities. This has also been observed by others.[33] However, the thermal conductivity of CO_2 is small at low densities, so the relative deviation becomes large for this reason.

The simulated thermal conductivities of CO_2 at 300 and 400 K are presented as a function of the pressure in Figure 5. Figure 5(a) for 300 K shows that all models predict well the experimental values. At 400 K (Fig. 5(b)), the computed values underestimate the experimental thermal conductivity of CO_2. This tendency is strengthened as the temperature rises, see Figures 6 and 7. All rigid models underestimate the thermal conductivity in these figures. This effect is stronger at high temperatures.

This tendency is quantified by the root mean square error (RMSE) computed from Eq. (12) and listed in Table III. For example, for the TraPPE model at 300 K the RMSE is only 6.8 $mW\,m^{-1}\,K^{-1}$. However, at 1000 K the RMSE has increased 6 times for the same model. As the consequence, the minimum error increases 9 times, up to 32.1%, at 1000 K.

Two main factors may contribute to this discrepancy. In the first place, the force fields of the rigid models that we have used were obtained at temperatures below the critical temperature of carbon dioxide (304 K). In spite of the good prediction, these models of the equation of state (Figure 3) may not have the wanted effect on a transport property like the thermal conductivity. Also, a rigid model may be too limited. Even CO_2 is a small molecule and the vibrational energy of CO_2 could be neglected up to 1000 K,[9,37] a possibility to bend or vibrate may have an impact on the simulated thermal conductivity.

To investigate the last factor further, we included two flexible models EPM2_Flex1 and EPM2_Flex2 as described

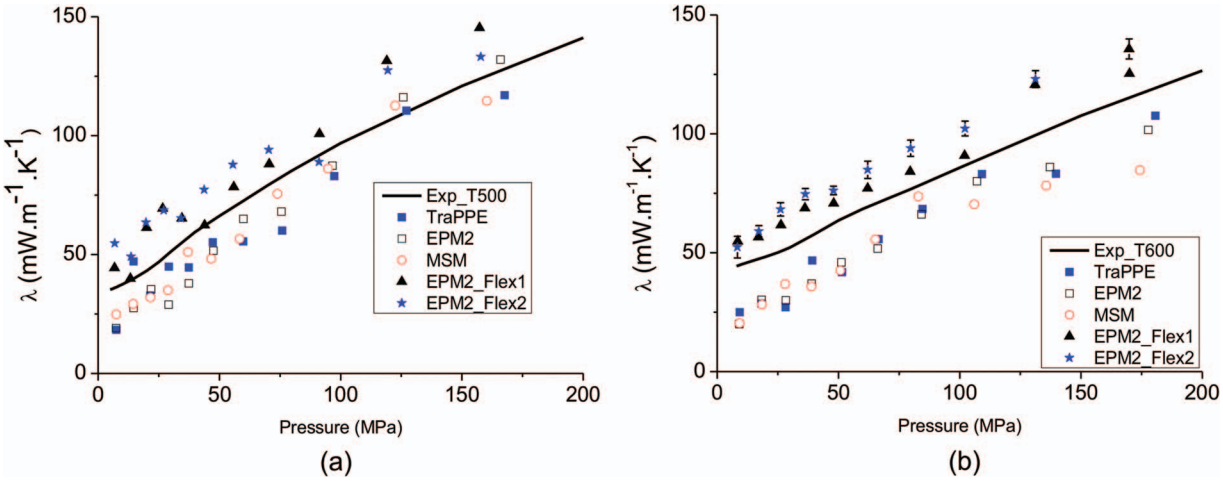

FIG. 6. Calculated thermal conductivity of rigid models (TraPPE, EPM2, MSM) and fully flexible models (EPM2_Flex1, EPM2_flex2) at T = 500 K (a) and T = 600 K (b). The straight line is experimental data taken from NIST data.[10]

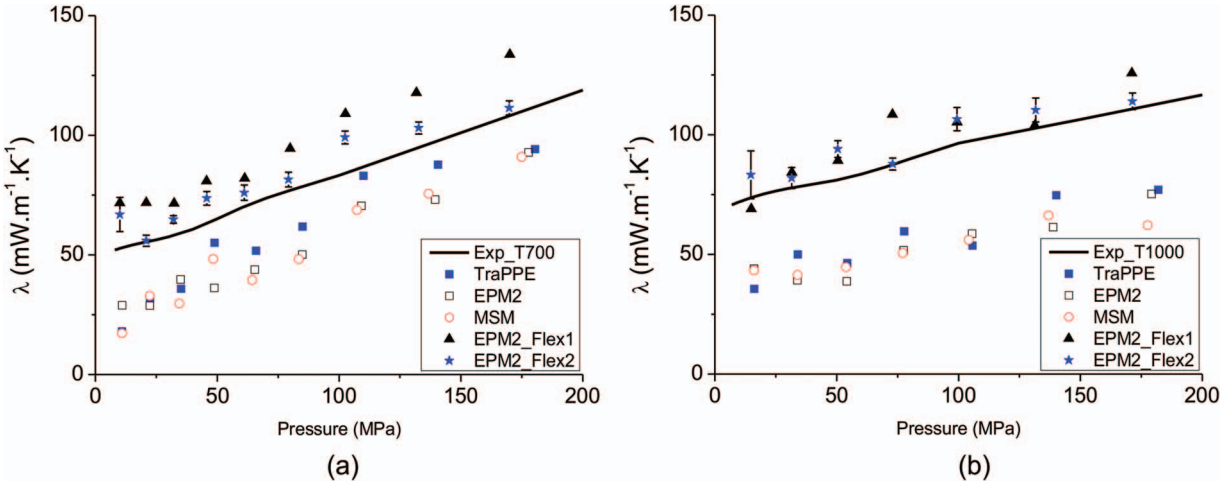

FIG. 7. Calculated thermal conductivity of rigid models (TraPPE, EPM2, MSM) and fully flexible models (EPM2_Flex1, EPM2_flex2) at T = 700 K (a) and T = 1000 K (b). The straight line is experimental data taken from NIST data.[10]

in Sec. II. The results are plotted along with the rigid model results in Figures 5–7. We see from Figs. 5–7 that the added possibility for bending and vibration in the molecule increases the thermal conductivity in all cases. On the whole, however, it leads to an overestimation of the experimental value.

The root mean square errors of all models for the whole temperature range are listed in Table III. In general, the TraPPE model is superior to the MSM or EPM2 models. At 300 K, the TraPPE model can forecast the thermal conductivity within an average error of 7 $mW\,m^{-1}\,K^{-1}$, while the EPM2 and MSM models show larger deviations, 15.4 and 14.3 $mW\,m^{-1}\,K^{-1}$, respectively. Using a semi-flexible or a full-flexible EMP2 model did not improve significantly the accuracy of the prediction.[7] The results predicted by these models were still 22%–30% from the experimental value. This suggests that the force fields need be optimized at higher temperatures, and possibly also for transport properties.

The observation is to some degree supported by Liang *et al.* who showed that fully flexible models with site-site interaction based on *ab initio* potential did not capture the thermal conductivity of CO_2 at density higher than 135 kg/m^3.[9] Also, a simple rigid model was able to reproduce the complex thermal conductivity of water, even at high temperature of 700 K.[33] At low temperatures, the rigid model of water overestimated thermal conductivity.[33]

In general, we have observed that the TraPPE model can better predict the thermal conductivity of CO_2 than the EPM2 and MSM-models do, and that the predictions are satisfactory at 300 K and low densities. All models yield an excellent prediction of the equation of state for CO_2, but they fail to predict experimental results at temperatures above 400 K. A clear effect of adding bond stretching and bond-bending is present in Figure 8. The rigid models are superior in low temperature region (below 600 K). However, at high temperature range (above 600 K), flexible models seem to be better. Using a better description of CO_2 bonding with Morse potential (EPM2_Flex2) already shows a slightly better results than a harmonic potential (EMP2_Flex1). However, a renewed evaluation of the force fields may also be needed to conclude on how to best reproduce the conductivity of CO_2 at high temperature. Adding flexibility to a rigid model (e.g., TraPPE) may require fully re-optimize the parameters of the force field. This will be included in our future work.

TABLE III. The root mean squared error (RMSE) (in $mW\,m^{-1}\,K^{-1}$) of the thermal conductivity of carbon dioxide, obtained by different rigid force field models in the temperature interval 300–1000 K. The value in the parentheses is the error (in %) from Eq. (13). The TraPPE model is better than the EPM2 and MSM models.

T (K)	TraPPE	EPM2	MSM	EPM2_Flex1	EPM2_Flex2
300	6.8 (3.7%)	15.4 (8.3%)	14.3 (6.6%)	21.3 (9.9%)	21.0 (9.7%)
400	8.6 (5.2%)	10.1 (6.1%)	10.2 (6.3%)	16.2 (10.1%)	14.7 (9.2%)
500	13.0 (10.1%)	13.2 (10.4%)	11.1 (8.9%)	14.4 (11.6%)	15.6 (12.6%)
600	16.9 (14.2%)	17.6 (14.9%)	20.6 (17.6%)	11.1 (9.7%)	16.7 (14.5%)
700	19.8 (17.7%)	24.1 (21.7%)	25.6 (23.3%)	19.3 (17.8%)	8.9 (8.2%)
1000	34.9 (30.8%)	38.5 (34.3%)	39.1 (34.9%)	11.2 (10.1%)	7.9 (7.2%)

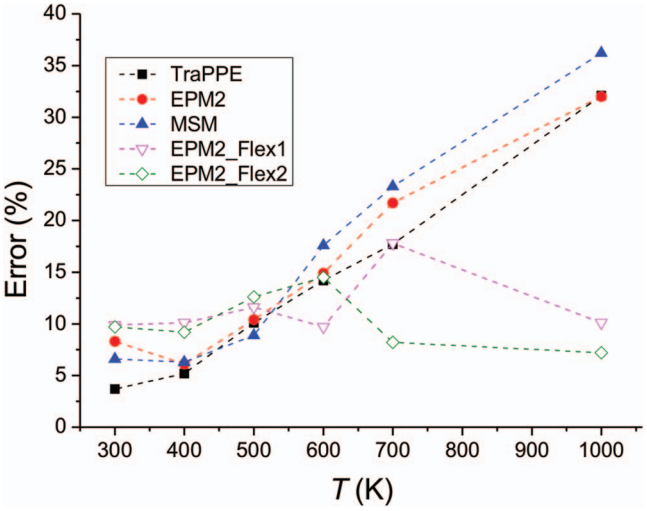

FIG. 8. Error (%) by Eq. (13) of rigid and flexible models in the prediction thermal conductivity of CO_2.

IV. CONCLUSIONS

We have employed nonequilibrium molecular dynamics simulation to explore the thermal conductivity of CO_2 of three popular rigid three-site models (TraPPE, EPM2, MSM) and two fully flexible models based on EPM2. It is remarkable that the models provide an excellent equation of state for CO_2 for low as well as high temperatures. The rigid models, especially the TraPPE model of CO_2, can predict the thermal conductivity of CO_2 within 5% error in a wide range of pressure for 300–400 K. This model can well be used to study heat and mass transfer in mixtures of CO_2 with CH_4 or H_2 for membrane separation processes near room temperature. The underestimation of the experimental results by all rigid models at high temperatures is probably due to a lack of optimization of the force fields at these conditions. In view of the importance of the properties of carbon dioxide, this deficiency should be mended.

ACKNOWLEDGMENTS

The authors acknowledge The Research Council of Norway RCN Project No. 209337 and The Faculty of Natural Science and Technology, Norwegian University of Science and Technology (NTNU) for financial support. The calculation power is granted by The Norwegian Metacenter for Computational Science (NOTUR).

[1]P. Bernardo, E. Drioli, and G. Golemme, Ind. Eng. Chem. Res. **48**, 4638 (2009).
[2]H. Yang, Z. Xu, M. Fan, R. Gupta, R. B. Slimane, A. E. Bland, and I. Wright, J. Environ. Sci. **20**, 14 (2008).
[3]X. He and M.-B. Hägg, J. Membr. Sci. **378**, 1 (2011).
[4]X. He, J. Arvid Lie, E. Sheridan, and M.-B. Hägg, Energy Proc. **1**, 261 (2009).
[5]Z. Yong, V. Mata, and A. R. E. Rodrigues, Sep. Purif. Technol. **26**, 195 (2002).
[6]D. Frenkel and B. Smit, *Understanding Molecular Simulation: From Algorithms to Applications* (Academic Press, 2002), Vol. 1.
[7]C. Nieto-Draghi, T. de Bruin, J. Pérez-Pellitero, J. B. Avalos, and A. D. Mackie, J. Chem. Phys. **126**, 064509 (2007).
[8]B. Wang, P. Cummings, and D. Evans, Mol. Phys. **75**, 1345 (1992).
[9]Z. Liang and H.-L. Tsai, Mol. Phys. **108**, 1285 (2010).
[10]G. Scalabrin, P. Marchi, F. Finezzo, and R. Span, J. Phys. Chem. Ref. Data **35**, 1549 (2006).
[11]T. T. Trinh, T. J. Vlugt, M. B. Hagg, D. Bedeaux, and S. Kjelstrup, Front. Chem. **1**, 38 (2013).
[12]S.-Y. Lee and S.-J. Park, J. Colloid Interface Sci. **389**, 230 (2013).
[13]L. Hamon, N. Heymans, P. L. Llewellyn, V. Guillerm, A. Ghoufi, S. Vaesen, G. Maurin, C. Serre, G. De Weireld, and G. D. Pirngruber, Dalton Trans. **41**, 4052 (2012).
[14]Y. Liu and J. Wilcox, Environ. Sci. Technol. **46**, 1940 (2012).
[15]X. Peng, D. Cao, and W. Wang, Chem. Eng. Sci. **66**, 2266 (2011).
[16]T. Trinh, D. Bedeaux, J.-M. Simon, and S. Kjelstrup, Chem. Phys. Lett. **612**, 214 (2014).
[17]C. Murthy, K. Singer, and I. McDonald, Mol. Phys. **44**, 135 (1981).
[18]J. G. Harris and K. H. Yung, J. Phys. Chem. **99**, 12021 (1995).
[19]J. J. Potoff and J. I. Siepmann, AIChE J. **47**, 1676 (2001).
[20]M. P. Allen and D. J. Tildesley, *Computer Simulation of Liquids* (Oxford University Press, 1989).
[21]S. Plimpton, P. Crozier, and A. Thompson, "LAMMPS-large-scale atomic/molecular massively parallel simulator," Sandia National Laboratories (2007).
[22]R. W. Hockney and J. W. Eastwood, *Computer Simulation using Particles* (CRC Press, 1988).
[23]M. Frisch, G. Trucks, H. Schlegel *et al.*, Gaussian 09, Revision B. 01, Gaussian, Inc., Wallingford, CT, 2009.
[24]A. D. Becke, Phys. Rev. A **38**, 3098 (1988).
[25]A. D. Becke, J. Chem. Phys. **98**, 5648 (1993).
[26]M. J. Frisch, J. A. Pople, and J. S. Binkley, J. Chem. Phys. **80**, 3265 (1984).
[27]See supplementary material at http://dx.doi.org/10.1063/1.4896965 for cut-off conditions, structures of CO_2, tabulated data of thermal conductivities, and equation of state.
[28]M. Bugel and G. Galliero, Chem. Phys. **352**, 249 (2008).
[29]F. Müller-Plathe, J. Chem. Phys. **106**, 6082 (1997).
[30]M. Zhang, E. Lussetti, L. E. de Souza, and F. Müller-Plathe, J. Phys. Chem. B **109**, 15060 (2005).
[31]B. Hafskjold, T. Ikeshoji, and S. K. Ratkje, Mol. Phys. **80**, 1389 (1993).
[32]I. Inzoli, J.-M. Simon, S. Kjelstrup, and D. Bedeaux, J. Colloid Interface Sci. **313**, 563 (2007).
[33]F. Römer, A. Lervik, and F. Bresme, J. Chem. Phys. **137**, 074503 (2012).
[34]I. Inzoli, J. M. Simon, D. Bedeaux, and S. Kjelstrup, J. Phys. Chem. B **112**, 14937 (2008).
[35]G. J. Martyna, M. L. Klein, and M. Tuckerman, J. Chem. Phys. **97**, 2635 (1992).
[36]M. Saharay and S. Balasubramanian, J. Phys. Chem. B **111**, 387 (2007).
[37]Z. Liang and H.-L. Tsai, Fluid Phase Equilib. **293**, 196 (2010).